RSC Advances

PAPER

View Article Online
View Journal | View Issue

Cite this: *RSC Adv.*, 2026, **16**, 7469

Chemical tailoring of heteroatom (P, S, Si) doping of COF-PEDOT for adsorption of paracetamol: perspective from DFT studies

Innocent E. Emeng, *[a] Uduak Luke,[b] Nguuma I. Gber,[c] Onyinyechi V. Ugochukwu,[d] Ambika Sundaravadivelu,[e] Gopinath Sampathkumar[f] and Musa Runde[dg]

The growing occurrence of pharmaceutical contaminants in aquatic systems has intensified the demand for advanced nanostructured materials capable of selective adsorption and removal of such pollutants. Paracetamol, a commonly used analgesic and antipyretic drug, is frequently detected in wastewater and poses severe ecological and health risks when accumulated in the water bodies and the soil. In this study, density functional theory (DFT) calculations were employed to investigate the structural, electronic, and adsorption behaviors of phosphorus (P), sulfur (S), and silicon (Si) doped COF-PEDOT frameworks for paracetamol adsorption. All geometries were optimized using the PBE0-D3/6-311G(d) basis set. The optimized structures exhibited minimal distortion after adsorption, indicating stable interactions between the adsorbate and the doped surfaces. Density of states (DOS) analysis revealed that heteroatom incorporation enhanced the electronic activity and reactivity of the complexes, while frontier molecular orbital (FMO) analysis showed a notable narrowing of the energy gap, confirming improved electron transfer capability. The ionization potential values (5.29–5.44 eV) remained within the range of moderately stable adsorbents. Natural bond orbital (NBO) analysis indicated that phosphorus doping produced the highest orbital stabilization energies, suggesting stronger donor–acceptor interactions. Adsorption energy calculations yielded negative values for all systems, confirming exothermic and thermodynamically favorable adsorption processes. Furthermore, quantum theory of atoms in molecules (QTAIM) and non-covalent interaction (NCI) analyses demonstrated the presence of weak but stable van der Waals and hydrogen-bond interactions governing paracetamol adsorption. The results demonstrate that tailored heteroatom doping can effectively tune the electronic and adsorption characteristics of COF-PEDOT frameworks. The P-, S-, and Si-doped systems exhibit enhanced sensitivity, stability, and reversibility, making them promising candidates for the selective adsorption of paracetamol from pharmaceutical contaminants in aquatic environments.

Received 29th October 2025
Accepted 22nd January 2026

DOI: 10.1039/d5ra08291a

rsc.li/rsc-advances

1 Introduction

Pharmaceutical contaminants have increasingly become a serious environmental concern due to their persistent release into aquatic ecosystems through various routes. Improper disposal of expired or unused drugs, hospital effluents, pharmaceutical manufacturing wastewater, and domestic sewage contribute significantly to the accumulation of these pollutants in surface and groundwater systems.[1] Paracetamol is a widely used pharmaceutical that is often detected in wastewater due to its incomplete removal in conventional treatment processes. Its persistence poses environmental and ecological risks, thereby creating a need for advanced materials with improved adsorption efficiency and selectivity. Paracetamol enters aquatic environments mainly through wastewater treatment plants that are often inefficient in removing such micropollutants.[2] Prolonged exposure to paracetamol-contaminated water has been reported to induce oxidative stress, endocrine disruption, and reproductive impairments in aquatic organisms. The prolonged exposure can alter antioxidant defense systems, leading to elevated reactive oxygen species (ROS), and cellular damage in fish and invertebrates. Paracetamol has also been shown to interfere with hormone regulation, affecting

[a]*Department of Human Physiology, University of Calabar, Calabar, Nigeria. E-mail: innocentekoro@gmail.com*
[b]*Department of Biochemistry, University of Uyo, Uyo, Nigeria*
[c]*Department of Microbiology, University of Calabar, Calabar, Nigeria*
[d]*Department of Chemistry, National Open University of Nigeria, Abuja, Nigeria*
[e]*Department of Chemistry, M. Kumarasamy College of Engineering (Autonomous), Karur - 639113, India*
[f]*Department of Chemistry, Chettinad College of Engineering & Technology, Karur - 639114, India*
[g]*Department of Research Analytics, Saveetha Dental College and Hospitals, Saveetha Institute of Medical and Technical Sciences, Saveetha University, Chennai, India*

growth, metabolism, and developmental processes.[3] Also, chronic accumulation of paracetamol in aquatic environments may impair fertility, and disrupt early life stages, thereby posing long-term risks to aquatic biodiversity and ecosystem stability in the long run. The persistence of paracetamol in water bodies also raises concerns for human health, as contaminated surface and groundwater can serve as sources of drinking water. Long-term human exposure to this contamination, even at trace levels, may contribute to cumulative toxicity, liver and kidney stress, and potential endocrine-related effects, emphasizing the need for effective removal strategies to protect both environmental and public health.[3] Moreover, its biotransformation products can accumulate in sediments and enter the food chain, posing indirect risks to human health such as liver dysfunction, carcinogenic effects, and antimicrobial resistance development.[4] On a global scale, pharmaceutical pollution is now recognized as a "planetary boundary threat," with studies indicating contamination in more than 70% of sampled rivers worldwide.[5] The collective ecological and health burden resulting from these contaminants further highlights the urgent need for advanced adsorption materials capable of effectively detecting and removing paracetamol and related pharmaceuticals from aquatic environments.

Recent research has focused on nanostructured materials as efficient adsorbents for pharmaceutical wastewater treatment. Among them, covalent organic frameworks (COFs) have attracted significant attention owing to their high surface area, chemical tunability, and porous architectures that enable selective adsorption of organic pollutants.[6] For instance, Niculescu, *et al.* (2023) reported the successful removal of paracetamol using a β-ketoenamine-linked COF with a maximum adsorption capacity of 284 mg g^{-1}, though the regeneration efficiency was limited after multiple cycles.[7] Similarly, Geng, Z. (2025) designed a sulfur-doped COF composite that exhibited enhanced adsorption performance toward non-steroidal anti-inflammatory drugs (NSAIDs) but showed poor stability under variable pH conditions.[8] Many other studies have integrated conductive polymers such as poly(3,4-ethylenedioxythiophene) (PEDOT) with COFs to form COF-PEDOT hybrids, improving electronic conductivity and adsorption kinetics performed by Cao, *et al.*,.[9] Despite these advances, the adsorption efficiency of these systems is often hindered by weak interactions between pollutant molecules and the adsorbent surface, limited recyclability, and insufficient understanding of the adsorption mechanisms at the molecular level.[10,11] Experimental work on COFs and PEDOT composites supports the feasibility of using hybrid conductive materials for pharmaceutical capture and sensing.[33] Tunable COF chemistries have been shown to affect paracetamol adsorption and degradation, while PEDOT-based films exhibit enhanced adsorbate interaction and electrochemical responsiveness.[34] These experimental demonstrations motivated this work's DFT-driven approach to map how heteroatom doping (P, S, Si) tunes adsorption energetics and electronic response, thereby providing molecular-level guidance to synthesis and performance optimization.

Despite the reported adsorption capabilities of existing materials, key limitations remain in understanding how electronic structure alteration governs paracetamol binding at the molecular level. This study addresses this gap by providing a first-principles framework for the rational design of high-performance COF-PEDOT adsorbents through systematic heteroatom (P, S, and Si) doping. Using density functional theory (DFT), it can be explained how targeted chemical tailoring alters charge distribution, frontier orbital alignment, and interfacial interaction strength with paracetamol. The comparative evaluation of multiple dopants enables identification of the most effective electronic environment for adsorption, offering mechanistic insight rather than empirical observation. By establishing direct structure–property–adsorption relationships, this work advances the design principles of COF-based nanomaterials and provides a transferable strategy for developing efficient, selective, and environmentally sustainable adsorbents for pharmaceutical wastewater remediation of paracetamol.

2 Method

The research was conducted using computational simulations *via* the density functional theory (DFT) as executed in the Gaussian 09 suite. All geometry optimizations were performed using the hybrid PBE0 functional with Grimme's D3 dispersion correction and a 6-311G(d) basis set (PBE0-D3/6-311G(d)), which ensures accurate treatment of the electronic structure and non-covalent interactions that are relevant to adsorption phenomena.[12] DFT was employed to study paracetamol adsorption on P-, S-, and Si-doped COF-PEDOT. This method accurately captures electronic interactions and adsorption energies, offering insights beyond those from semi-empirical or classical methods used in previous reports. The COF-PEDOT framework was selected as the model nanomaterial due to its combined structural rigidity, extended π-conjugation, and intrinsic electrical conductivity, which are desirable properties for adsorption and sensing applications. Conductive polymer–COF hybrids such as PEDOT-functionalized frameworks have been shown to exhibit enhanced charge transport and stronger electronic coupling with aromatic pharmaceutical molecules, resulting in improved adsorption sensitivity and signal transduction (Zhang *et al.*, *J. Mater. Chem. C*, 2021, **9**, 11234–11243). Heteroatom doping was introduced to deliberately tune the electronic structure and adsorption behavior of COF-PEDOT. Phosphorus was selected because P-doping introduces electron-rich sites and localized charge polarization, which can enhance donor–acceptor interactions with oxygen-containing molecules such as paracetamol (Wang *et al.*, *RSC Adv.*, 2020, **10**, 27645–27653). Sulphur was chosen due to its high polarizability and ability to participate in non-covalent interactions, including hydrogen bonding and π–sulphur interactions, which have been reported to improve adsorption strength in sensing materials (Liu *et al.*, *New J. Chem.*, 2019, **43**, 17821–17829). Silicon doping was included to evaluate the effect of a less electronegative heteroatom, as Si incorporation has been shown to modulate band structure and surface reactivity without significantly disrupting the framework geometry (Chen *et al.*, *Phys. Chem. Chem. Phys.*, 2021, **23**, 14678–14686). A low

Table 1 Calculated bond length and bond angle in COF-PEDOT-based compounds before and after adsorption of paracetamol

Compound before adsorption	Bonding atoms	Bond angle atoms	Bond-length (Å)	Bond-angle (Å)	Compound-after adsorption	Bond-length (Å)	Bond-angle (Å)
COF-PEDOT	S130–C127	S130–C127–C137	1.75	122.400	PCL-COF-PEDOT	1.75	122.49
	O69–B75	O69–B75–O71	1.38	118.91		1.38	118.86
	C116–C115	C116–C115–S113	1.37	109.62		1.37	109.60
P@COF-PEDOT	P159–O32	O32–P159–C93	1.67	98.44	PCL-P@COF-PEDOT	1.68	99.32
	S129–C125	S129–C125═C127	1.75	109.62		1.75	109.66
	O1–B9	O1–B9–C7	1.38	118.72		1.38	118.83
	P159–O32	P159–O32–B2	1.67	125.70		1.68	125.12
S@COF-PEDOT	S112–C114	S112–C114–C125	1.75	121.92	PCL-S@COF-PEDOT	1.70	121.79
	B43–O38	O38–B43–C36	1.38	120.65		1.38	119.93
	C130═C131	C130═C131–O132	1.33	123.95		1.33	123.96
	O68–B74	C72–B74–O68	1.38	121.56		1.38	122.63
Si@COF-PEDOT	C93–Si159	C93–Si159–O32	1.86	110.14	PCL-Si@COF-PEDOT	1.85	109.83
	O40–B43	O40–B43–C36	1.37	120.68		1.37	119.71
	S142–C136	S142–C136–C126	1.75	121.78		1.75	121.55
	B30–O67	B30–O67–Si159	1.37	122.80		1.36	123.04

dopant concentration corresponding to single-atom substitution was employed to preserve the structural integrity of the COF-PEDOT framework while enabling direct comparison of electronic and adsorption properties across all systems, consistent with previous DFT studies on heteroatom-doped porous materials (Sun *et al.*, *RSC Adv.*, 2018, **8**, 38967–38975). Dopant atoms were positioned at chemically active sites within the framework to maximize electronic perturbation and interaction with the adsorbate. Paracetamol was optimized independently at the same level of theory to ensure consistency. Adsorption energies, frontier molecular orbital properties, NBO charge transfer, and QTAIM/NCI analyses were subsequently used to elucidate the nature and strength of interactions between paracetamol and pristine and doped COF-PEDOT systems. These analyses provide direct insight into how heteroatom doping influences binding strength and electronic response upon adsorption. The optimized Cartesian coordinates of all structures are provided in the SI to ensure reproducibility.

3 Results and discussion

3.1 Geometry optimization

Geometry optimization provides fundamental insights into how paracetamol (PCL) interacts with COF-PEDOT and heteroatom-doped (P, S, Si) COF-PEDOT frameworks. Structural responses such as shifts in bond lengths and bond angles reflect the degree of electronic rearrangement and the nature of interaction occurring upon adsorption.[13,14] Across all systems, the optimized structures before and after PCL adsorption showed only minor geometric perturbations, indicating that adsorption does not distort the COF-PEDOT backbone but still induces measurable electronic adjustments at the active sites. In pristine COF-PEDOT, the characteristic C–S bond (S130–C127) retained its length at 1.75 Å before and after adsorption, signifying structural strength of the thiophene unit. The B–O bonds (*e.g.*, O69–B75), which define the COF linker environment, also remained within the expected 1.36–1.39 Å range, with negligible deviation after adsorption.[15] These results suggest that adsorption primarily occurs through weak non-covalent forces without altering the main COF framework. Phosphorus doping introduced more pronounced local changes. The P–O bond (P159–O32) increased slightly from 1.67 Å to 1.68 Å following the adsorption of paracetamol there was an angle shift from 98.44° to 99.32°. These distortions imply enhanced electron redistribution around the phosphorus site, consistent with P acting as an electron-rich doping center capable of interacting with the phenolic –OH and amide groups of PCL.[16]. In the S-doped system, subtle deviations were also observed, such as the B74–O68–C72 angle increasing by approximately 1°. Sulfur's polarizability allows greater flexibility in structural response, enabling moderate charge rearrangement during adsorption. For Si-doped COF-PEDOT, slight reductions in the Si–O bond length (1.86 Å → 1.85 Å) and bond angles reflect silicon's tendency to form flexible, partially polar bonds. This mild structural adjustment supports weaker binding relative to P- and S-doped systems. Overall, geometry analysis suggests the following trend in local structural responsiveness during adsorption: P-doped > S-doped > Si-doped > pristine COF-PEDOT. This ranking correlates strongly with later electronic property analysis and explains why phosphorus-doped materials demonstrate the most favorable adsorption characteristics (Table 1 and Fig. 1).

3.2 Electronic properties

3.2.1 Density of state (DOS) analysis. The density of states (DOS) plots generated using GaussSum[17] were analyzed to elucidate how heteroatom doping modifies the electronic structure of COF-PEDOT upon adsorption of paracetamol. Rather than focusing solely on the band gap, emphasis is placed on the total DOS distribution, the density and continuity of electronic states, and the adsorption-induced redistribution of occupied and virtual orbitals, which collectively govern surface reactivity and adsorption strength. For the PCL-COF-PEDOT

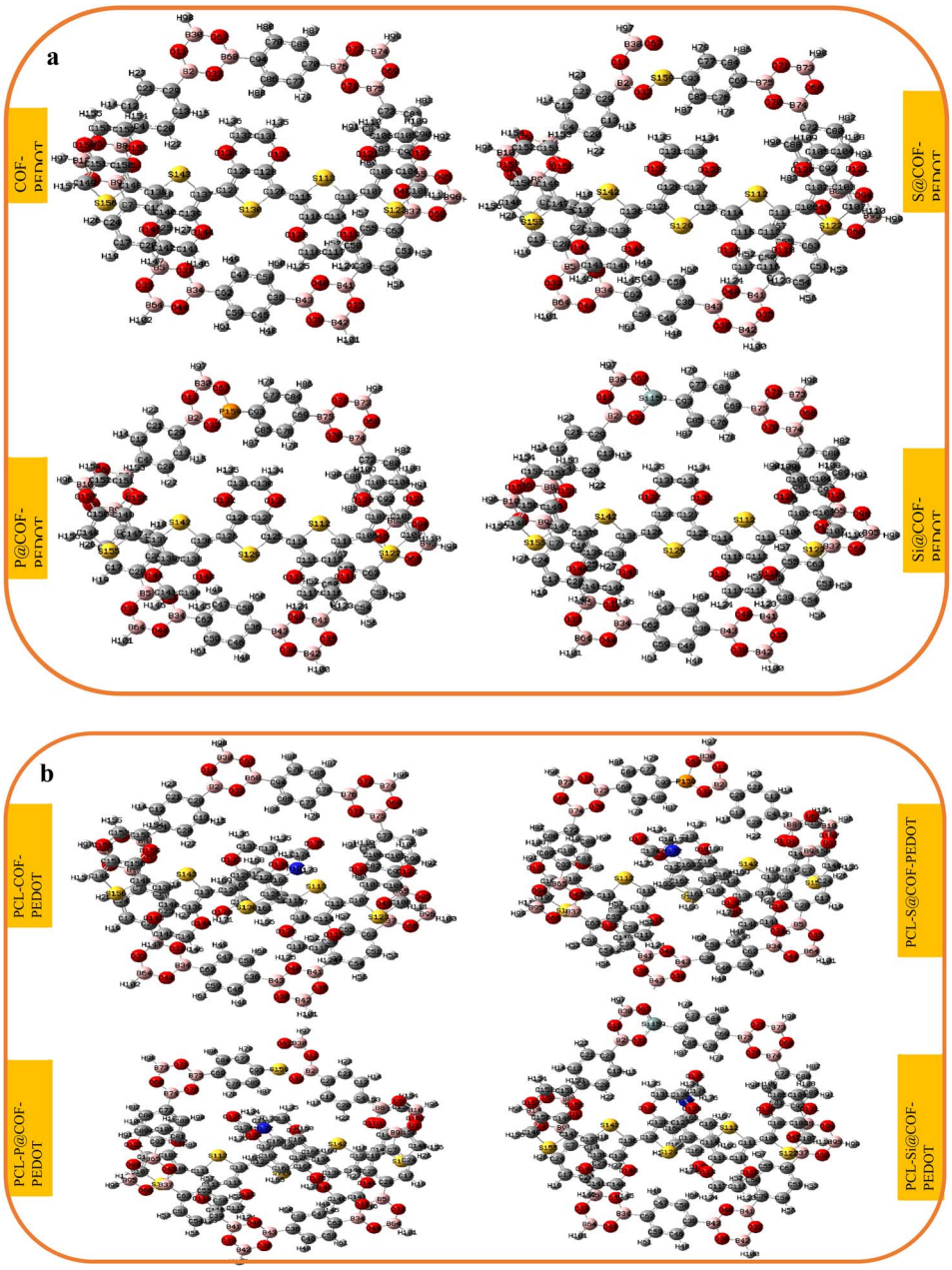

Fig. 1 (a) Structural representations of the studied compounds before adsorption of paracetamol. (b) Structural representations of the studied compounds after adsorption.

system, the total DOS exhibits a continuous and well-distributed profile across the valence region, dominated by carbon-derived π states originating from the conjugated PEDOT framework. The relatively high DOS intensity in the occupied region indicates effective orbital availability for interaction with paracetamol. The presence of noticeable unoccupied states close to the occupied manifold suggests feasible electronic communication between the adsorbent and adsorbate, supporting π–π stacking and weak charge redistribution upon adsorption. Overall, the DOS profile reflects a balanced electronic structure that favors moderate interaction without excessive localization. In the phosphorus-doped system (PCL-P@COF-PEDOT), the total DOS shows a discernible redistribution of states, particularly near the frontier orbital region. Compared to the pristine system, the DOS intensity becomes more concentrated, indicating enhanced localization of electronic states around the adsorption site. This redistribution suggests that phosphorus introduces electronically active centers that strengthen orbital overlap with paracetamol. The improved alignment of occupied and virtual states enhances adsorption-induced electronic coupling, reflecting stronger surface–adsorbate interactions. For the sulphur-doped system (PCL-S@COF), the DOS profile retains the overall continuity of the pristine framework but exhibits a more uniform spread of

electronic states across both occupied and unoccupied regions. The total DOS intensity remains relatively high, implying preserved conjugation and efficient electronic delocalization. This balance between localization and delocalization indicates that sulphur doping enhances electronic adaptability of the surface, facilitating adsorption while maintaining the structural electronic integrity of COF-PEDOT. In the silicon-doped system (PCL-Si@COF), the DOS plot reveals noticeable broadening of electronic states and a reduction in DOS intensity near the frontier region compared to phosphorus and sulphur doping. This behavior indicates that silicon doping introduces more delocalized electronic states, which, while significantly altering the overall electronic structure, may reduce the density of chemically active orbitals directly involved in adsorption. Consequently, the interaction with paracetamol is electronically stabilized but less focused at specific adsorption sites. Beyond band gap considerations, an important parameter evident from the DOS plots is the degree of state overlap between occupied and virtual orbitals, which reflects the potential for adsorption-induced electronic redistribution. Systems exhibiting higher DOS density and better continuity near the frontier region demonstrate stronger surface reactivity. Additionally, the total DOS peak intensity serves as an indicator of available electronic states for interaction, with sharper and denser peaks suggesting enhanced adsorption capability. Comparatively, the pristine COF-PEDOT system displays moderate DOS intensity and balanced state distribution, resulting in reasonable interaction with paracetamol. Phosphorus doping leads to increased localization and higher effective DOS density near the adsorption-relevant region, favoring stronger electronic coupling. Sulphur doping offers an optimal compromise between state delocalization and density, maintaining high DOS intensity while enhancing electronic flexibility. Silicon doping, although inducing significant electronic restructuring, results in broader and less concentrated DOS features, which may limit effective adsorption interactions (Fig. 2).

3.2.2 Natural bond orbital. The Natural Bond Orbital (NBO) analysis is a computational method used to describe the

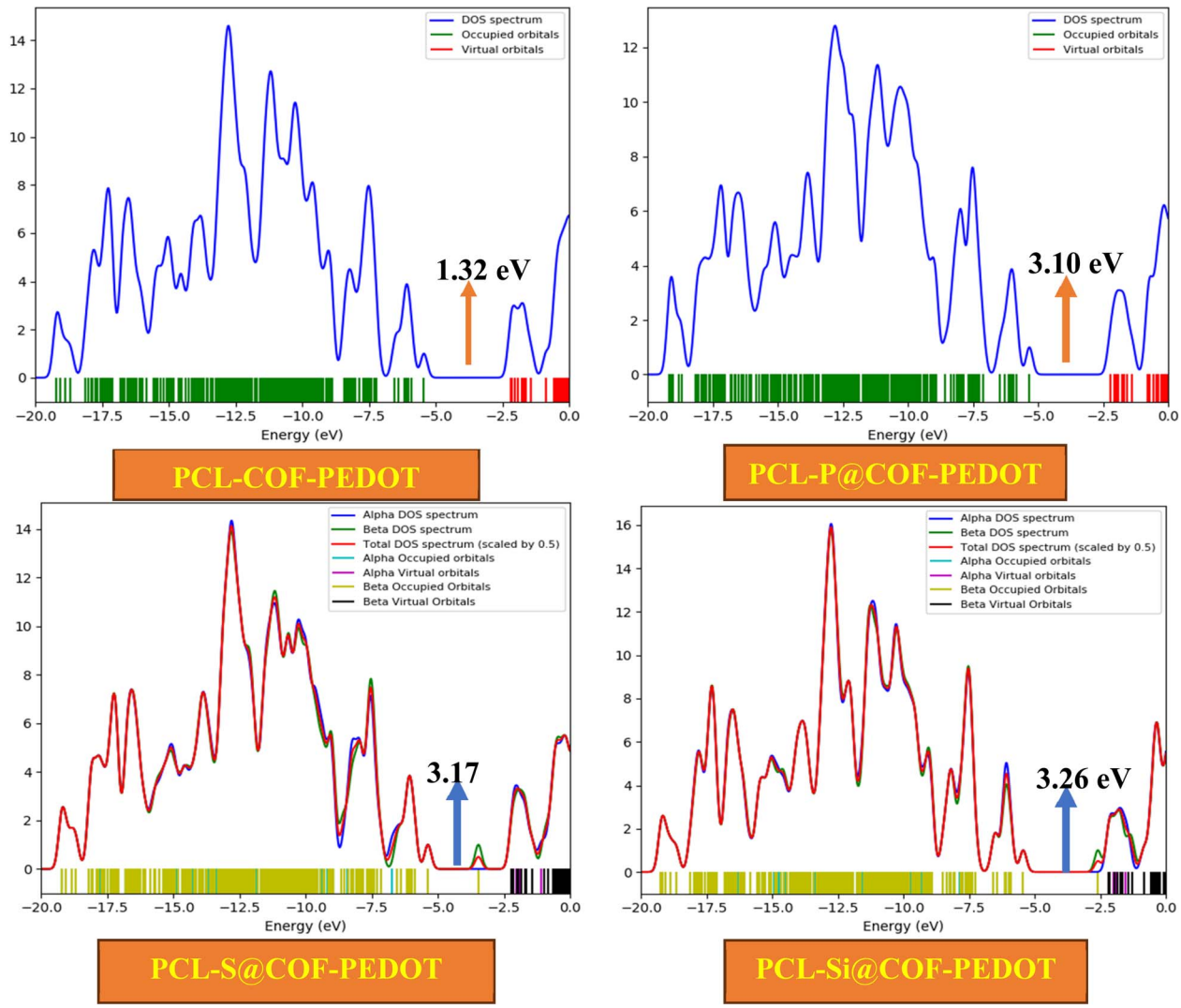

Fig. 2 Total density of states (TDOS) of the pristine and heteroatom-doped system.

electronic structure of molecules. The computational method helps in presenting insights into several electronic properties such as electron density distribution and the charge transfer between bonding (σ) and antibonding (σ*) orbitals, which significantly influence molecular stability.[18] These interactions are quantified using the second-order perturbation energy ($E^{(2)}$). In the donor and acceptor interaction framework, electron donor (i) and acceptor (j) orbitals are identified based on interactions between the bonding and antibonding orbitals. These interactions are primarily responsible for charge transfer between atoms or molecular splits.[30] The second-order perturbation energy is calculated using the calculation (eqn (1)) below:

$$E^{(2)} = q\mathrm{i}\frac{\left(\left(F_{\mathrm{ij}}\right)^{2}\right)}{E_{(\mathrm{i})} - E_{(\mathrm{j})}} \quad (1)$$

where F_{ij} represents the off-diagonal Fock matrix element, $E_{(i)} - E_{(j)}$ are the diagonal elements, and $E^{(2)}$ represent the second order perturbation energy of the chemical system. According to previous literature, higher values of $E^{(2)}$ correspond to stronger interactions between the donor and acceptor orbitals, which have a direct impact on the molecular stability and adsorption properties.[19] The NBO analysis of heteroatom-doped PCL@COF-PEDOT complexes in Table 2 provides detailed insight into their stability and electronic interactions. The NBO analysis of the heteroatom-doped PCL@COF-PEDOT revealed critical insight into the donor–acceptor interaction with the formed paracetamol complexes. The interaction was primarily between lone pair (LP) electrons of oxygen atoms and the antibonding σ* orbitals on the doped nanostructured framework, thereby explaining the various stabilizations among the systems. In the PCL-P@COF-PEDOT complex, the interaction between the lone pair on oxygen atom O67 and the antibonding orbital σB30–O67 was the most pronounced donor–acceptor interaction, with a stabilization energy of (E^2) of 277.56 kcal mol^{-1}. This interaction is followed by other powerful LP → σ transitions from O66 and O38 to antibonding orbitals with boron centres, with second-order stabilization energies of 263.59 kcal mol^{-1} and 258.97 kcal mol^{-1}, respectively. These high E^2 values show a clear charge delocalization and strong orbital overlap, suggesting that phosphorus doping enhances electron density restructuring, thereby significantly enhancing the stabilization of the adsorbed system. In the sulphur-doped complex, (PCL-S@COF-PEDOT), the stabilization energies were generally lower, with values such as 217.96 kcal mol^{-1} for the LP-O32 → σB2 interaction and 148.98 kcal mol^{-1} for LP-O11 → σB30. Despite these being considerable, they are notably weaker than those observed in the phosphorus-doped complex. This reduced E^2 values indicates that sulphur introduces moderately strong but less delocalized interactions. This is consistent with sulphur's electronic configuration and polarizability, which favours softer, more flexible interactions.[20] In the PCL-Si@COF-PEDOT system, the perturbation energy (E^2) values were moderate, with the strongest interactions such as LP-O66 → σB37 and LP-O33 → σB5 showing stabilization energies of 132.47 kcal mol^{-1} and 131.22 kcal mol^{-1}, respectively. These silicon-doped interactions are the weakest among the three systems, this indicates that silicon doping results in the least extent of electronic delocalization and orbital interaction with the adsorbed paracetamol. This weak interaction is attributed to silicon's larger atomic radius and lower electronegativity, which can reduce the extent of orbital overlap and Fock matrix elements.[21] The NBO results clearly showed that the phosphorus doping system yielded the most electronically stabilized complex, followed by sulphur, and then silicon. This emphasizes that phosphorus contributes significantly to enhanced charge transfer and interaction strength, which is favourable for sensing applications where orbital hybridization and electronic perturbation are critical.

3.2.3 Quantum descriptors

3.2.3.1 Frontier molecular orbital (FMO) and global reactivity descriptor analysis. To obtain a comprehensive understanding of the electronic reactivity and adsorption behavior of COF-PEDOT and its heteroatom-doped derivatives toward paracetamol, frontier molecular orbital (FMO) analysis was combined with global quantum reactivity descriptors derived from HOMO and LUMO energies. These parameters collectively provide insight into stability, charge-transfer propensity, and adsorption-induced electronic modifications.[22] The HOMO energy represents the electron-donating ability of the adsorbent. As shown in Table 3, HOMO values for all systems fall within the range of −5.29 to −5.44 eV, indicating good intrinsic electronic stability. Upon PCL adsorption, a general downward shift in HOMO energies is observed, exemplified by pristine COF-PEDOT, which shifts from −5.29 eV to −5.44 eV after adsorption. This decrease signifies enhanced electronic

Table 2 Donor–acceptor, transition, stabilization energies (E^2) of heteroatom-doped PCL@COF-PEDOT complexes

Compound	Donor (i)	Acceptor (j)	$E^{(2)}$ kcal mol^{-1}	$E_{(j)} - E_{(i)}$ a. u.	F(i, j) a. u.	Transition
PCL-P@COF-PEDOT	LP-O67	σ*B30–O67	277.56	0.780	0.418	LP → σ*
	LP-O66	σ*LP-B37	263.59	0.590	0.357	LP → σ*
	LP-O38	σ*LP-B37	258.97	0.580	0.351	LP → σ*
PCL-S@COF-PEDOT	LP-O11	σ*LP-B30	148.98	0.60	0.384	LP → σ*
	LP-O32	σ*LP-B2	217.96	0.85	0.548	LP → σ*
	LP-O66	σ*LP-B37	132.05	0.59	0.357	LP → σ*
PCL-Si@COF-PEDOT	LP-O66	σ*LP-B37	132.47	0.59	0.358	LP → σ*
	LP-O33	σ*LP-B5	131.22	0.58	0.355	LP → σ*
	LP-O6	σ*LP-B43	121.14	0.59	0.343	LP → σ*

Table 3 Computed electronic key parameters for HOMO and LUMO energies, and other quantum parametric descriptors of the various heteroatoms doped PCL-COF-PEDOT systems (all computed parametric energy values are represented in electron volts (eV))

Compound	HOMO (eV)	LUMO (eV)	Energy gap (eV)	Σ	H	$(-\mu)$	ω	E_{FL}
COF-PEDOT	−5.29	−2.17	3.12	0.32	1.56	−3.73	4.46	3.73
P@COF-PEDOT	−5.40	−2.08	3.32	0.30	1.66	−3.74	4.21	3.74
S@COF-PEDOT	−5.33	−2.22	3.11	0.32	1.56	−3.78	4.59	3.78
Si@COF-PEDOT	−5.30	−2.06	3.24	0.31	1.62	−3.68	4.18	3.68
PCL-COF-PEDOT	−5.44	−2.18	3.26	0.31	1.63	−3.81	4.46	3.81
PCL-P@COF-PEDOT	−5.33	−2.23	3.10	0.32	1.55	−3.78	4.61	3.78
PCL-S@COF-PEDOT	−5.37	−2.21	3.17	0.32	1.58	−3.79	4.54	3.79
PCL-Si@COF-PEDOT	−5.44	−2.18	3.26	0.31	1.63	−3.81	4.46	3.81

stabilization and partial electron donation from the framework to the adsorbate, a behavior commonly associated with physisorption accompanied by mild charge redistribution. The LUMO energies, which describe the electron-accepting capacity of the systems, remain relatively invariant (−2.06 to −2.23 eV) before and after adsorption. This limited variation suggests that the ability of the frameworks to accept electrons is largely preserved upon PCL binding. Such stability in LUMO levels indicates that adsorption does not significantly perturb the conduction characteristics of the COF-PEDOT backbone, which is desirable for reusable sensing and adsorption materials. The HOMO–LUMO energy gap (ΔE) is a critical indicator of chemical reactivity and charge-transfer efficiency. Smaller ΔE values correspond to higher polarizability and enhanced electronic communication between the adsorbent and adsorbate. Prior to adsorption, ΔE values range from 3.11 to 3.32 eV. Following PCL adsorption, most systems exhibit a reduction in ΔE, particularly in doped frameworks. For instance, P@COF-PEDOT shows a decrease from 3.32 eV to 3.10 eV after adsorption, reflecting increased reactivity and improved charge-transfer interactions induced by PCL binding. The global softness (Σ) and chemical hardness (η) further support this trend. Chemical hardness, defined as half of the energy gap, reflects resistance to charge transfer, whereas softness is its inverse measure and indicates the ease of electron cloud deformation. As presented in Table 3, η values decrease slightly upon PCL adsorption (*e.g.*, from 1.66 to 1.55 eV for P-doped systems), while Σ shows a corresponding marginal increase. This complementary behavior confirms that adsorption enhances the electronic responsiveness of the systems, facilitating charge exchange at the interface. The negative chemical potential ($-\mu$), which approximates the electronegativity of the system, provides insight into the tendency of the framework to attract electrons. The relatively consistent $-\mu$ values (−3.68 to −3.81 eV) indicate that both pristine and doped COF-PEDOT systems maintain a strong driving force for electron exchange. Slightly more negative values observed after PCL adsorption suggest stabilization of the electronic system and increased affinity for charge redistribution during adsorption. The electrophilicity index (ω) quantifies the ability of a system to accept electrons. Higher ω values are associated with stronger electrophilic character and improved interaction with nucleophilic species. In Table 3, ω values show a modest increase after PCL adsorption, particularly for doped systems such as PCL-P@COF-PEDOT (ω = 4.61 eV). This enhancement implies that adsorption strengthens the electrophilic nature of the framework, thereby favoring stronger adsorbate–adsorbent interactions.[23] Finally, the Fermi level (E_{FL}) reflects the position of the electronic equilibrium level and plays a crucial role in charge-transfer processes. The observed shift in E_{FL} toward more negative values after adsorption (*e.g.*, from 3.73 to 3.81 eV for pristine COF-PEDOT) suggests electron transfer from the adsorbent to the adsorbate. Such shifts are indicative of adsorption-induced electronic perturbations and further confirm the occurrence of interfacial charge redistribution. Since the work function is defined as the energy difference between the vacuum level and the Fermi level, this shift indicates a corresponding change in the work function upon paracetamol adsorption, which directly influences surface reactivity and adsorption strength.

3.3 Adsorption studies

Previous studies have emphasized that adsorption energy is a key parameter in evaluating the interaction strength between adsorbent materials and pollutant molecules such as pharmaceuticals.[24] In environmental remediation, particularly for paracetamol removal, adsorption energy provides critical insight into how effectively an adsorbent surface can capture and retain target molecules while maintaining structural stability and potential reusability.[25] Materials exhibiting moderately strong adsorption energies are often preferred, as they ensure a balance between high adsorption capacity and facile desorption or regeneration, which are essential for sustainable wastewater treatment operations.[26]

In this work, adsorption energies were considered for paracetamol interacting with the various heteroatom-doped PCL@COF-PEDOT systems, with dopants including phosphorus, sulfur, and silicon. From the adsorption studies (see Table 4), it was observed that all the systems yielded negative adsorption energies, this confirms that the interaction was exothermic, hence it is thermodynamically favorable. Among the three complexes, PCL-P@COF-PEDOT and PCL-S@COF-PEDOT exhibited the same adsorption energies of −1.170 eV. This similar negative adsorption energies suggest that both dopants form moderately strong non-covalent interactions with paracetamol, making them capable of sensing paracetamol

Table 4 Adsorption energies of heteroatom-doped PCL@COF-PEDOT complexes for paracetamol sensing

System	E (complex)	E (adsorbent)	E (adsorbate)	E (a.u)	E (eV)
PCL-P@COF-PEDOT	−7873.527	−7397.752	−475.732	−0.043	−1.170
PCL-S@COF-PEDOT	−7930.232	−7454.457	−475.732	−0.043	−1.170
PCL-Si@COF-PEDOT	−7821.685	−7345.917	−475.732	−0.036	−0.980

molecule effectively, while allowing for reversibility. On the other hand, PCL-Si@COF-PEDOT had a lower adsorption energy of −0.980 eV, this lower adsorption energy can be attributed to silicon atomic radius, which limit the orbital overlap and ultimately leads to a reduced charge transfer with paracetamol. The finding from the adsorption studies showed that the introduction of heteroatoms enhanced the sensitivity of COF-PEDOT for paracetamol. Although this study is purely theoretical, the DFT predictions in this work are consistent with experimental trends reported for COF- and PEDOT-based adsorbents. Tunable COFs have been shown experimentally to control adsorption and degradation of paracetamol through tailored framework chemistry.[35] PEDOT-containing composites have also demonstrated strong polymer–drug interactions and favorable electrochemical adsorption behavior in practical films, supporting the concept that conductive polymer integration improves adsorbate affinity.[36] Furthermore, COF adsorbents have been used successfully to capture pharmaceutical pollutants in aqueous media, providing real-world context for the adsorption energies we report.[34] These studies suggest that our predicted trend (P ≈ S > Si in adsorption strength) can guide targeted synthesis of doped COF-PEDOT composites for paracetamol removal and sensing in wastewater treatment.

3.4 Visual studies

3.4.1 Quantum theory of atoms in molecules (QTAIM) analysis. The Quantum Theory of Atoms in Molecules (QTAIM), as developed by Bader, was employed to elucidate the nature of the intermolecular interactions governing the COF-PEDOT interface and to evaluate how heteroatom doping modulates these interactions upon paracetamol adsorption.[27,28] QTAIM is based on the topological analysis of the electron density distribution, where bonding interactions are identified through bond critical points (BCPs) and their associated descriptors, including electron density ($\rho(r)$), Laplacian of electron density ($\nabla^2\rho(r)$), kinetic energy density ($G(r)$), potential energy density ($V(r)$), total energy density ($H(r)$), ellipticity (ε), and the ratio $G(r)/|V(r)|$. Among these parameters, $\nabla^2\rho(r)$ and $H(r)$ are particularly useful for classifying interaction types. Positive values of $\nabla^2\rho(r)$ together with positive $H(r)$ are indicative of closed-shell, non-covalent interactions, whereas negative $H(r)$ values suggest partial covalent character, and simultaneous negative $\nabla^2\rho(r)$ and $H(r)$ correspond to strong covalent bonding.[29] For the pristine PCL-COF-PEDOT system, the identified BCPs (Table 5) exhibit low electron density values ($\rho(r) \approx 0.0034$–0.0061 a.u.), positive Laplacians, and positive total energy densities. These features confirm that the interaction between COF and PEDOT is dominated by weak non-covalent forces, such as van der Waals and hydrogen-bond-like contacts as presented in Fig. 3. The relatively high $G(r)/|V(r)|$ ratios (>1) further support the closed-shell nature of these interactions. Structurally, this implies that PCL adsorption does not significantly distort the COF-PEDOT framework but is stabilized through weak interfacial contacts. Upon phosphorus (P) doping, notable changes are observed in the QTAIM descriptors. In the PCL-P@COF-PEDOT system, the H52–C174 interaction (CP 324) shows reduced electron density but a lower $G(r)/|V(r)|$ ratio (~1.50) compared to the pristine system, indicating relatively enhanced interaction strength. This suggests that P doping increases local polarization within the framework, thereby promoting stronger adsorbate–framework interactions. Additionally, the appearance of a C–C interaction (C105–C181) with higher $\rho(r)$ values indicates that P incorporation subtly reorganizes the electronic structure, strengthening certain interfacial contacts without transitioning into covalent bonding. Sulfur (S) doping introduces further modulation of the interaction landscape. In the PCL-S@COF-PEDOT system, the S129–H52 and O175–H78 interactions exhibit distinct QTAIM signatures. Although the S–H interaction shows very low electron density, the O–H contact displays

Table 5 Quantum theory of atoms in molecules (QTAIM) topological descriptors of non-covalent interactions in COF-PEDOT systems (all quantities measured in a.u)

Systems	Bond	CP	$\rho(r)$	$\nabla^2\rho(r)$	$G(r)$	$V(r)$	$H(r)$	$\frac{G(r)}{\lvert V(r)\rvert}$	E_{FL}	λ_1	λ_2	λ_3	λ_1/λ_3	ε
PCl-COF-PEDOT	H_{60}–H_{166}	235	0.0034	0.0157	0.0025	−0.0012	0.0013	2.083	0.0074	−0.0031	0.0221	−0.0023	1.3478	0.0508
	C_{170}–H_{49}	241	0.0061	0.0341	0.0062	−0.0038	0.0023	1.631	0.0090	−0.0072	0.0471	−0.0058	1.2414	0.2354
PCl-P@COF-PEDOT	H_{52}–C_{174}	324	0.0014	0.0052	0.0009	−0.0006	0.0004	1.500	0.0029	−0.0007	0.0015	0.0044	−1.636	−1.496
	C_{105}–C_{181}	369	0.0071	0.0198	0.0047	−0.0044	0.0025	1.760	0.0252	−0.0042	−0.0010	0.0251	−0.167	3.0615
PCl-S@COF-PEDOT	S_{129}–H_{52}	78	0.0003	0.0018	0.0003	−0.0001	0.0001	3.000	0.0002	0.0011	−0.0001	0.0008	1.375	−1.181
	O_{175}–H_{78}	248	0.0151	0.0690	0.0153	−0.0134	0.0019	1.141	0.0291	−0.0207	0.1107	−0.021	0.985	0.0124
PCl-Si@COF-PEDOT	O_{45}–O_{78}	261	0.0112	0.0529	0.0110	−0.0088	0.0022	1.250	0.0212	0.0695	−0.0077	−0.0087	−7.988	0.1239
	O_{143}–S_{122}	244	0.0101	0.0484	0.0099	−0.0077	0.0021	1.285	0.1882	0.0622	−0.0061	−0.0077	−8.077	0.2498

relatively higher $\rho(r)$ (0.0151 a.u.) and a lower $G(r)/|V(r)|$ ratio (1.141), pointing to comparatively stronger hydrogen-bond-like interactions. This indicates that S doping enhances the hydrogen-bonding capability of the framework, likely due to increased electron delocalization around sulfur sites, which facilitates stronger adsorption while maintaining non-covalent character. In the Si-doped system (PCL-Si@COF-PEDOT), the QTAIM descriptors reveal more pronounced structural reorganization. The O–O and O–S interactions exhibit higher electron density values ($\rho(r) \approx 0.010$–0.011 a.u.) and lower $G(r)/|V(r)|$ ratios (~1.25–1.29), suggesting relatively stronger non-covalent interactions compared to both pristine and other doped systems. The large magnitude of eigenvalue ratios (λ_1/λ_3) and increased ellipticity values further indicate enhanced anisotropy and electron density deformation at the interaction regions. Structurally, this implies that Si doping induces stronger polarization effects within the COF-PEDOT matrix, thereby reinforcing interfacial stability and improving adsorption efficiency.

3.4.2 Non-covalent interaction (3D plots). The NCI analysis is an important parameter that unveils the nature of interaction and bonding type on a system.[30] It also accounts for the nature of interaction that occurs between the COF and PEDOT together with the doped atoms, which have great effect on the system. The NCI also visualizes weak interaction by introspecting the reduced density gradient RDG, connoting to the electron density.[31] In Fig. 4, the result of the 3D RDG plots of the NCI analysis provide reliable information. These interactions are denoted by colors wherein red color depicts steric repulsion, which is mathematically interpreted by the expression $((\lambda_2)\ \rho(r)) > 0$, hence ensuring high sensitivity while maintaining sufficient reversibility and selectivity. The green color denotes van der Waals interaction given as $((\lambda_2)\ \rho(r)) \approx 0$, and blue color for strong attractive force where the second eigenvalues of Hessian is $((\lambda_2)\ \rho(r) < 0)$ is observed with a negative sign. We observe a similar trend among the complexes in Fig. 4. For complex PCL-COF-PEDOT, PCL-P@COF-PEDOT, PCL-S@COF-PEDOT and PCL-Si@COF-PEDOT, in that there is a saturation of van der Waals bonding in the center of the interaction while the other

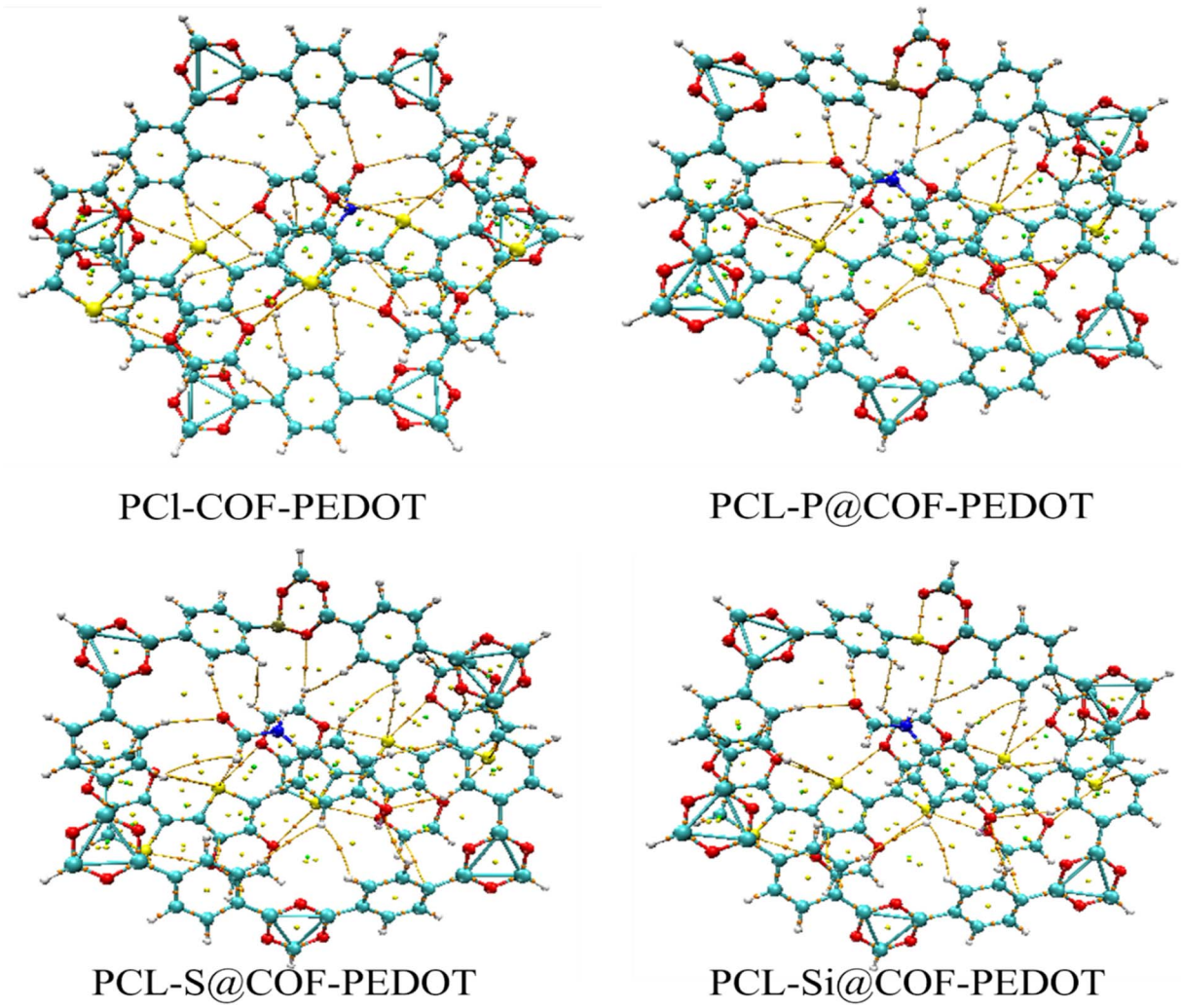

Fig. 3 Quantum Theory of Atoms in Molecules (QTAIM) molecular graphs of COF-PEDOT and doped complexes showing bond critical points (BCPs) and bond paths corresponding to non-covalent interactions.

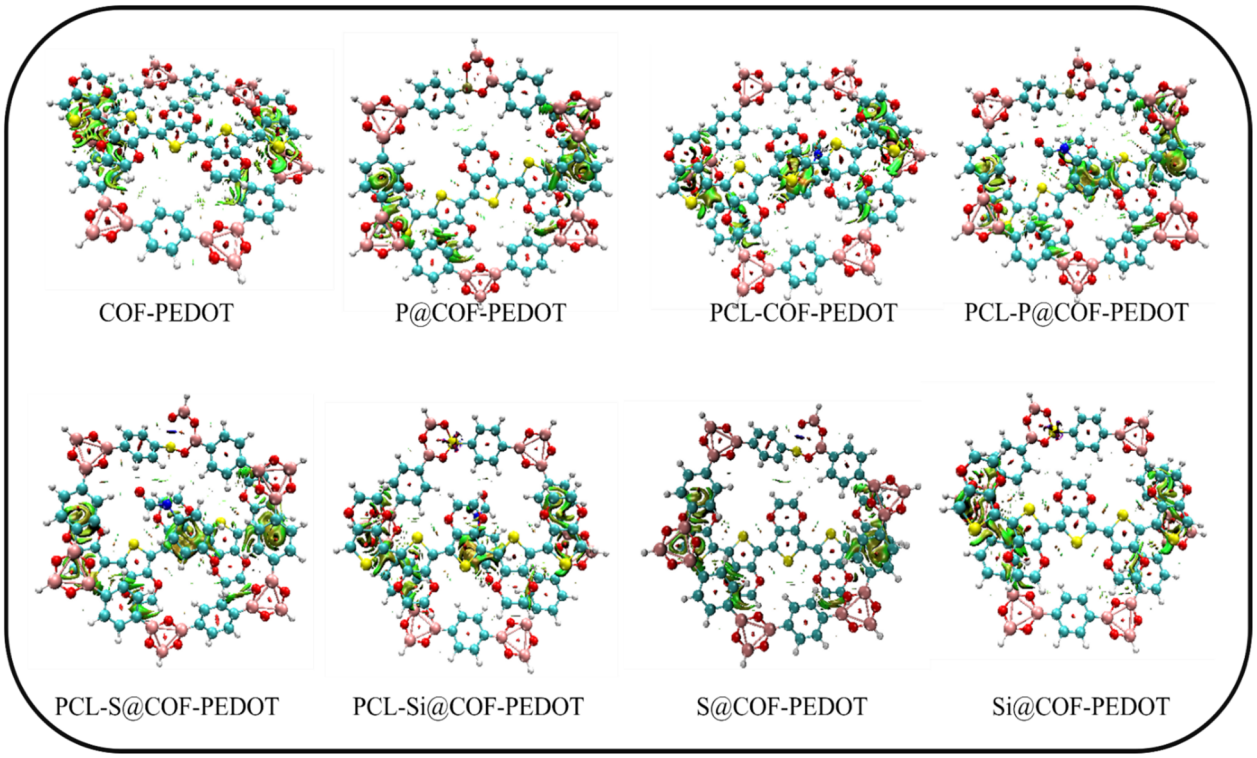

Fig. 4 NCI isosurfaces of COF-PEDOT and doped systems highlighting regions of weak attractive and repulsive interactions.

counterparts have more van der Waals interaction at both ends. This result support facile electron transfer from both reacting molecules, making it a reliable candidate for environmental remediation.[32] All the studied complexes are consistent with the nature of van der Waals forces and a bit of steric repulsive forces among the rings due to resonance stability.

4 Future perspectives and challenges

The theoretical insights obtained in this study provided a clear guidance for the experimental design of heteroatom-doped COF-PEDOT materials for paracetamol adsorption. The predicted influence of P, S, and Si dopants on electronic structure and adsorption strength suggests that controlled heteroatom incorporation can be used to optimize adsorption performance. These materials show potential for practical applications in wastewater treatment filters, membranes, and sensing platforms. However, challenges remain in achieving precise dopant control, ensuring long-term stability in aqueous environments, and validating adsorption capacity and regeneration through experiments. Addressing these aspects will be essential for translating the present DFT predictions into real-world applications.

5 Conclusions

This study investigated the chemical modification of covalent organic framework poly(3,4-ethylenedioxythiophene) (COF-PEDOT) composites through heteroatom (P, S, and Si) doping to enhance their adsorption capability toward paracetamol in environmental systems. Using first-principles density functional theory (DFT) calculations, the structural, electronic, and adsorption properties of the doped systems were thoroughly analyzed. Geometry optimization revealed only minor angular distortions following paracetamol adsorption, indicating that the complexes remained structurally stable throughout the interaction process.

Electronic structure analyses, including density of states (DOS) and frontier molecular orbital (FMO) evaluations, provided further insights into the reactivity trends of the doped frameworks. The DOS profiles showed that heteroatom incorporation enhanced the electronic activity of COF-PEDOT, with the Si-doped system exhibiting the most pronounced Fermi-level shift (−5.9 eV), suggesting stronger orbital delocalization and improved adsorption affinity. Similarly, FMO analysis indicated that heteroatom doping effectively narrowed the HOMO–LUMO energy gaps, signifying increased chemical reactivity and stability. The ionization potentials of all materials ranged between 5.29 eV and 5.44 eV, consistent with literature-reported values (4.5–6.0 eV) for moderately stable adsorbents. Natural bond orbital (NBO) results further demonstrated that phosphorus doping produced the highest orbital stabilization energies, reflecting stronger donor–acceptor interactions. Adsorption energy calculations revealed negative values for all systems, confirming that the adsorption of paracetamol was exothermic and thermodynamically favorable. Among the three doped structures, PCL-P@COF-PEDOT and PCL-S@COF-PEDOT exhibited comparable adsorption energies (−1.170

eV), suggesting moderately strong and reversible noncovalent interactions suitable for reusable adsorbent applications. Conversely, the Si-doped complex (PCL-Si@COF-PEDOT) showed a relatively lower adsorption energy (−0.980 eV), likely due to silicon's larger atomic radius, which limits orbital overlap and charge transfer efficiency. Topological (QTAIM) and non-covalent interaction (NCI) analyses confirmed the presence of weak but stable van der Waals interactions across all systems, indicating that adsorption primarily occurs through physisorption rather than chemisorption.

Although the present study focuses on the adsorption mechanisms of paracetamol on P, S, and Si-doped COF-PEDOT *via* DFT calculations, repeatability and cycling studies are important to assess the practical stability and reusability of these materials. Future experimental investigations are encouraged to perform adsorption–desorption cycling tests and replicate adsorption measurements to validate the computational predictions and ensure consistent performance. Collectively, these findings establish that heteroatom doping effectively tunes the electronic configuration and adsorption characteristics of COF-PEDOT frameworks. The incorporation of phosphorus, sulfur, and silicon atoms enhances both sensitivity and reversibility, making the doped COF-PEDOT materials promising candidates for the selective adsorption of paracetamol from pharmaceutical contaminants in aquatic environments.

Author contributions

Innocent E. Emeng conceptualized the research, drafted the initial manuscript, contributed in the adsorption studies and approved the final version of the manuscript. Uduak Luke and Nguuma I. Gber carried out the computational modeling, data validation and preparation of figures and tables. Onyinyechi V. Ugochukwu contributed to the interpretation of the electronic structure. Ambika Sundaravadivelu assisted in literature review. Gopinath Sampathkumar contributed in editing for intellectual content. Musa Runde supervised the entire project and provided critical revisions.

Conflicts of interest

There are no conflicts of interest to declare.

Data availability

Additional computational data are available upon request from the corresponding author.

All data supporting the findings of this study are included within the manuscript and its supplementary information (SI). Supplementary information: optimized Cartesian coordinates of all structures obtained at the DFT level used in this work. See DOI: https://doi.org/10.1039/d5ra08291a.

References

1 N. Zaidi, M. A. Mir, S. K. Chang, N. Abdelli, S. M. Hasnain, M. A. Ali Khan and K. Andrews, Pharmaceuticals and personal care products as emerging contaminants: environmental fate, detection, and mitigation strategies, *Int. J. Environ. Anal. Chem.*, 2025, 1–29.
2 I. U. Islam, A. N. Qurashi, A. Adnan, A. Ali, S. Malik, F. Younas and E. Yabalak, Bioremediation and adsorption: strategies for managing pharmaceutical pollution in aquatic environment, *Water, Air, Soil Pollut.*, 2025, **236**(9), 579.
3 W. K. Wardhani, E. S. Soedjono, H. S. Titah and M. A. Mardyanto, Pharmaceutical emerging micropollutants potential in septic tanks: its fate and transport study in Indonesia – a literature review, *Environ. Qual. Manage.*, 2024, **34**(1), e22176.
4 P. Loffler, B. I. Escher, C. Baduel, M. P. Virta and F. Y. Lai, Antimicrobial transformation products in the aquatic environment: global occurrence, ecotoxicological risks, and potential of antibiotic resistance, *Environ. Sci. Technol.*, 2023, **57**(26), 9474–9494.
5 H. P. H. Arp, A. Gredelj, J. Gluge, M. Scheringer and I. T. Cousins, The global threat from the irreversible accumulation of trifluoroacetic acid (TFA), *Environ. Sci. Technol.*, 2024, **58**(45), 19925–19935.
6 K. Patra, S. Dey, C. Solanki, A. Sengupta and V. K. Mittal, Harnessing advanced porous materials, covalent organic frameworks, and porous organic polymers as next-generation porous frameworks for targeted removal of emerging water contaminants, *ACS Appl. Eng. Mater.*, 2025, **3**(5), 1130–1165.
7 A. G. Niculescu, B. Mihaiescu, D. E. Mihaiescu, T. Hadibarata and A. M. Grumezescu, An updated overview of magnetic composites for water decontamination, *Polymers*, 2024, **16**(5), 709.
8 Z. Geng, A highly sensitive fluorescent detection method utilizing B and S co-doped graphene quantum dots for ibuprofen analysis, *Alexandria Eng. J.*, 2025, **112**, 17–25.
9 C. Cao, Q. Chen, R. Suizu and K. Awaga, Critical transition to a highly conductive state through PEDOT oligomer percolation in redox-active COFs, *J. Mater. Chem. C*, 2024, **12**(9), 3072–3076.
10 D. Bakowies and O. A. von Lilienfeld, Density functional geometries and zero-point energies in ab initio thermochemical treatments of compounds with first-row atoms (H, C, N, O, F), *J. Chem. Theory Comput.*, 2021, **17**(8), 4872–4890.
11 Z. Ullah, H. J. Kim, Y. S. Mary, N. Belboukhari, K. Sekkoum, A. Kraimi and H. W. Kwon, Unlocking the potential of ovalene: a dual-purpose sensor and drug enhancer, *J. Mol. Liq.*, 2023, **377**, 121540.
12 G. Sanyal, M. Kandasamy, B. Mondal, A. Seetharaman and B. Chakraborty, Pd-anchored VSe_2 for glucose sensing: prediction from first principle simulations, *Surf. Interfaces*, 2024, **54**, 105235.

13 K. W. Qadir, M. D. Mohammadi and H. Y. Abdullah, Modelling gas adsorption onto Al12(Zn)N12 surfaces: a theoretical study of CH4, CO, CO2, H2O, N2, NH3, NO, NO2, O2, and SO2 interactions, *Comput. Theor. Chem.*, 2025, **1244**, 115063.

14 R. Zhao, B. Li, S. Chen, B. Zhang, J. Chen, J. Sun and X. Ma, Intertwined role of mechanism identification by DFT-XAFS and engineering considerations in the evolution of P adsorbents, *Sci. Total Environ.*, 2024, **946**, 174159.

15 R. Rahimi and M. Solimannejad, A novel pentagonal BCN monolayer for sensing and drug delivery of nitrosourea and hydroxyurea anticancer drugs: a DFT outlook, *Mater. Sci. Semicond. Process.*, 2024, **173**, 108109.

16 I. S. Oliveira, M. S. Garcia, N. M. Cassani, A. L. Oliveira, L. C. Freitas, V. K. Bertolini and C. Abbehausen, Exploring antiviral and antiparasitic activity of gold N-heterocyclic carbenes with thiolate ligands, *Dalton Trans.*, 2024, **53**(47), 18963–18973.

17 T. Takeshita and D. Kinoshita, Evaluation of darrow red–organosilane composite as a photosensitizer for application in dye-sensitized zinc oxide photocatalysts: DFT and TD-DFT studies, *J. Mol. Model.*, 2022, **28**(12), 407.

18 H. Gu, F. Wang, S. Chen, J. Lan, J. Wang, C. Pei and J. Gong, Suppressing Jahn-Teller distortion of MnO2 via B-Ni dual single-atoms integration for methane catalytic combustion, *Nat. Commun.*, 2025, **16**(1), 1008.

19 S. Suthar and K. C. Mondal, Unveiling the anomaly of reduction of carborane-bis-silylene-stabilised silylone/germylone leading to unusual oxidation of Si0/Ge0 to SiI/GeI with EDA-NOCV analyses, *Chem.–Eur. J.*, 2024, **30**(10), e202303355.

20 W. A. Mahdi, A. Alhowyan and A. J. Obaidullah, A DFT insight into the potential of cycloparaphenylenes as efficient sensors for detecting paracetamol, *Sci. Rep.*, 2025, **15**(1), 8150.

21 W. Dong, J. Xing, Q. Chen, Y. Huang, M. Wu, P. Yi and B. Xing, Hydrogen bonds between the oxygen-containing functional groups of biochar and organic contaminants significantly enhance sorption affinity, *Chem. Eng. J.*, 2024, **499**, 156654.

22 A. U. Rahman, M. K. Rokunuzzaman, D. M. Saaduzzaman, M. S. Rahman, M. Amin, S. M. Hasan and M. K. U. Sikder, Designing nitride-derived fullerenes X20N20 (X = B, Al, and Ga) for the effective delivery of the cardiovascular drug felodipine: a DFT study, *Nanoscale*, 2025, **17**(42), 24755–24772.

23 Y. Liang, L. Feng, X. Liu, Y. Zhao, Q. Chen, Z. Sui and N. Wang, Enhanced selective adsorption of NSAIDs by covalent organic frameworks via functional group tuning, *Chem. Eng. J.*, 2021, **404**, 127095.

24 L. Wu, Z. Dai, H. Fu, M. Shen, L. Cha, Y. Lin and B. Lu, Multiple electron transfers enable high-capacity cathode through stable anionic redox, *Adv. Mater.*, 2025, **37**(9), 2416298.

25 A. Zamani, F. F. Sead, I. Kaur, A. Kubaev, S. T. Hamedani and H. Majedi, DFT analysis of dimethyl fumarate interactions with B12N12 and B24 nanoclusters for enhanced anticancer drug delivery, *Comput. Theor. Chem.*, 2025, **1247**, 115168.

26 R. K. Sharma, A. Srivastava, U. Punia, R. Bansal, P. Prajapat, G. Gupta and S. K. Srivastava, Multifunctioning graphene oxide capping layer for highly efficient and stable PEDOT:PSS–silicon hybrid solar cells, *Sustainable Energy Fuels*, 2024, **8**(20), 4799–4812.

27 S. A. Halim, A. B. El-Meligy, A. M. El-Nahas and S. H. El-Demerdash, DFT study and natural bond orbital (NBO) population analysis of 2-(2-hydroxyphenyl)-1-azaazulene tautomers and their mercapto analogues, *Sci. Rep.*, 2024, **14**(1), 219.

28 H. Louis, L. P. Ifediora, O. C. Enudi, T. O. Unimuke, F. C. Asogwa and Y. L. Moshood, Evaluation of the excited state dynamics, photophysical properties, and the influence of donor substitution in a donor-π-acceptor system, *J. Mol. Model.*, 2021, **27**(10), 284.

29 A. Mahmood, A. Irfan, F. Ahmad and M. R. S. A. Janjua, Quantum chemical analysis and molecular dynamics simulations to study the impact of electron-deficient substituents on electronic behavior of small molecule acceptors, *Comput. Theor. Chem.*, 2021, **1204**, 113387.

30 H. A. Rizwan, M. U. Khan, A. Anwar, S. Alharthi and M. A. Amin, First theoretical framework of Al9N9 and B9N9 nanorings for unveiling their unique detection and sensing potential for SF6 decomposition gases (H2S, SO2, SOF2, and SO2F2): toward real-time gas sensing in high-voltage power systems, *RSC Adv.*, 2025, **15**(25), 20020–20039.

31 S. Noreen, S. H. Sumrra, A. U. Hassan, M. Afzaal, A. Y. E. Elnaggar, I. H. E. Azab and M. H. Mahmoud, A DFT and molecular correlational analysis on newly designed silicon-carbide quantum dots with extended acceptors for their photovoltaic performance, *Silicon*, 2025, 1–13.

32 Q. Wang, S. Lian, C. Guo, X. Gao, Y. Dou, C. Song and J. Lin, The chemical adsorption effect of surface-enhanced Raman spectroscopy of nitrobenzene and aniline using density functional theory, *Spectrochim. Acta, Part A*, 2022, **279**, 121428.

33 X. Liu, D. Huang, C. Lai, G. Zeng, L. Qin, H. Wang and S. Chen, Recent advances in covalent organic frameworks (COFs) as a smart sensing material, *Chem. Soc. Rev.*, 2019, **48**(20), 5266–5302.

34 A. Mellah, S. P. Fernandes, R. Rodríguez, J. Otero, J. Paz, J. Cruces and L. M. Salonen, Adsorption of pharmaceutical pollutants from water using covalent organic frameworks, *Chem.–Eur. J.*, 2018, **24**(42), 10601–10605.

35 F. Liu, Z. Ma, Y. Deng, M. Wang, P. Zhou, W. Liu and D. Ma, Tunable covalent organic frameworks with different heterocyclic nitrogen locations for efficient Cr(VI) reduction, Escherichia coli disinfection, and paracetamol degradation under visible-light irradiation, *Environ. Sci. Technol.*, 2021, **55**(8), 5371–5381.

36 J. H. Viteri, N. Cotolan, L. Barbu-Tudoran and G. L. Turdean, A paracetamol-poly(3,4-ethylenedioxythiophene) composite film for drug release studies, *Mater. Today Commun.*, 2023, **34**, 105084.